

SNAD Transient Miner: Finding Missed Transient Events in ZTF DR4 using k-D trees

P. D. Aleo^{a,b}, K. L. Malanchev^{a,c}, M. V. Pruzhinskaya^c, E. E. O. Ishida^d,
E. Russeil^d, M. V. Kornilov^{c,e}, V. S. Korolev^{f,g}, S. Sreejith^h, A. A. Volnovaⁱ,
G. S. Narayan^{a,j}

^a*Department of Astronomy, University of Illinois at Urbana-Champaign, 1002 West Green Street, Urbana, 61801, IL, USA*

^b*Center for AstroPhysical Surveys (CAPS) Fellow, National Center for Supercomputing Applications, USA*

^c*Lomonosov Moscow State University, Sternberg Astronomical Institute, Universitetsky pr. 13, Moscow, 119234, Russia*

^d*Université Clermont Auvergne, CNRS/IN2P3, LPC, Clermont-Ferrand, F-63000, France*

^e*National Research University Higher School of Economics, 21/4 Staraya Basmannaya Ulitsa, Moscow, 105066, Russia*

^f*Central Aerohydrodynamic Institute, 1 Zhukovskiy st, Zhukovskiy, Moscow Region, 140180, Russia*

^g*Moscow Institute of Physics and Technology, 9 Institutskiy per., Dolgoprudny, Moscow Region, 141701, Russia*

^h*Physics Department, Brookhaven National Laboratory, Upton, NY, 11973, USA*

ⁱ*Space Research Institute of the Russian Academy of Sciences (IKI), 84/32 Profsoyuznaya Street, Moscow, 117997, Russia*

^j*Center for AstroPhysical Surveys (CAPS), National Center for Supercomputing Applications, 1205 West Clark Street, Urbana, 61801, IL, USA*

Abstract

We report the automatic detection of 11 transients (7 possible supernovae and 4 active galactic nuclei candidates) within the Zwicky Transient Facility fourth data release (ZTF DR4), all of them observed in 2018 and absent from public catalogs. Among these, three were not part of the ZTF alert stream. Our transient mining strategy employs 41 physically motivated features extracted from both real light curves and four simulated light curve models (SN Ia, SN II, TDE, SLSN-I). These features are input to a k-D

Email address: paleo2@illinois.edu (P. D. Aleo)

tree algorithm, from which we calculate the 15 nearest neighbors. After pre-processing and selection cuts, our dataset contained approximately a million objects among which we visually inspected the 105 closest neighbors from seven of our brightest, most well-sampled simulations, comprising 92 unique ZTF DR4 sources. Our result illustrates the potential of coherently incorporating domain knowledge and automatic learning algorithms, which is one of the guiding principles directing the SNAD team. It also demonstrates that the ZTF DR is a suitable testing ground for data mining algorithms aiming to prepare for the next generation of astronomical data.

Keywords: Transient sources (1851), Time domain astronomy (2109), Supernovae (1668), Active galactic nuclei (16)

PACS: 0000, 1111

2000 MSC: 0000, 1111

1. Introduction

The volume and complexity of astronomical data have drastically increased with the arrival of large scale astronomical surveys, the state of the art being the Zwicky Transient Facility¹ (ZTF), which generates ~ 1.4 TB of data per night of observation (Graham et al., 2019). This new data paradigm has forced astronomers to search for automatic tools which can enable classification and discovery within such large datasets.

Traditional supervised machine learning algorithms rely on the availability of large representative training samples, which are not feasible in astronomy (Ishida et al., 2019b). Classification requires spectroscopic confirmation, which is an expensive and time consuming process, thus limiting and biasing the population of objects for which classes can be known. Moreover, even with spectroscopy, labels can be incorrect, making unsupervised methods powerful tools. The use of machine learning algorithms opens the possibility of studying larger populations within each class as well as their application in further scientific analysis. A particularly well-studied example of this scenario is the task of supernova (SN) photometric classification. Since their first use as standardizable candles (Riess et al., 1998; Perlmutter et al., 1999) a lot of effort has been devoted to the development, and

¹<https://www.ztf.caltech.edu/>

adaptation, of machine learning classifiers which may enable purely photometric supernova cosmology (see Ishida et al., 2019b, and references therein). This covers a large variety of learning algorithms (e.g. Lochner et al., 2016; Boone, 2019; Sooknunan et al., 2021; Alves et al., 2021), including deep (e.g., Muthukrishna et al., 2019; Pasquet et al., 2019; Möller et al., 2020; Villar et al., 2020; Allam and McEwen, 2021; Burhanudin et al., 2021) and adaptive (e.g., Ishida et al., 2019a; Kennamer et al., 2020) learning techniques. These deep learning approaches leverage recurrent neural networks (RNNs, Muthukrishna et al., 2019; Möller et al., 2020), RNN-based autoencoders (Sadeh, 2020; Villar et al., 2021), Temporal Convolutional Networks (TCNs, Muthukrishna et al., 2021), and more.

This new direction towards data driven approaches has also benefited from increasingly more realistic simulations. Given the sparse availability of confirmed classifications, simulations have filled the gap when real data are not available. They have been used to compare results from different classifiers in the context of data challenges, like SNPhotCC (Kessler et al., 2010) and PLAsTiCC (Hložek et al., 2020), as well as used to replace training samples in transfer learning scenarios (e.g., Pasquet et al., 2019). In all such attempts, large volumes of simulations are used to infer statistical properties of different classes which can allow bulk data classification. In parallel, unsupervised learning techniques have been used for clustering (e.g., Krone-Martins and Moitinho, 2014; Ralph et al., 2019; Pera et al., 2021) and anomaly detection (e.g., Villar et al., 2020; Storey-Fisher et al., 2021; Martínez-Galarza et al., 2021) without the need of labels. In this context, simulations have also been used to validate the proposed algorithms (e.g., Villar et al., 2021).

The SNAD² team has been continuously working in the development of anomaly detection algorithms which are able to prove their efficiency in real data while incorporating domain knowledge in the machine learning model – thus tailoring it according to the scientific interest of the expert (e.g., Pruzhinskaya et al., 2019; Aleo et al., 2020; Malanchev et al., 2021; Ishida et al., 2021). In this work, we present a hybrid approach for mining transients in large astronomical datasets, specifically ZTF DR4; moreover, our methodology can also be applied to the nightly ZTF alert-stream via time-domain brokers like ANTARES (Matheson et al., 2021) and FINK (Möller

²<https://snad.space/>

et al., 2021). Ultimately, our analysis still focuses on performance on real data; however, we use a few simulated light curves as a guide to identify transients in a large dataset mostly comprised of variable stars (Chen et al., 2020).

We describe the data, simulations, and pre-processing steps in Section 2. The simulation-to-data matching algorithm is described in Section 3 and results are shown in Section 4. Our conclusions are outlined in Section 5.

2. Data

2.1. ZTF DR4

ZTF is a northern sky survey stationed at Mount Palomar. It uses a 48-inch Schmidt telescope equipped with a 47 deg² camera, with primary science objectives including the physics of SN and relativistic explosions, multi-messenger astrophysics, SN cosmology, active galactic nuclei (AGN), tidal disruption events (TDE), stellar variability and Solar System objects (Graham et al., 2019). The survey started on March 2018 and, during its initial phase, has observed around a billion objects (Bellm et al., 2019). It is employed as a testing ground for the next generation of large scale surveys like the Vera Rubin Observatory Legacy Survey of Space and Time (LSST, LSST Science Collaboration et al. 2009). For this work, we use the survey’s fourth data release (DR4), made public on December 9, 2020³.

2.2. Simulations

We create realistic ZTF simulations using SNANA (Kessler et al., 2009), a catalog-level light curve simulator which includes effects due to telescope characteristics and observational conditions. We adopt ZTF data release 3 cadence and magnitude error distribution (see Chatterjee et al. 2021 for details). Among the template models originally developed for the Photometric LSST Astronomical Time-series Classification Challenge (PLAsTiCC, Kessler et al., 2019; Hložek et al., 2020), we used only type SN Ia, SN II, SLSN-I, and TDE.

For each model, we generated $\sim 50,000$ ⁴ simulations and imposed a series of quality cuts (SNR > 5, magnitude limit, $m < 21.5^m$, and a minimum of

³<https://www.ztf.caltech.edu/news/dr4>

⁴This number results in a small but sufficient portion of well-sampled simulations located in the bright tail of the peak magnitude distribution.

100 observations in each of the zr - and zg -bands). We then chose, among the surviving objects, the seven brightest light curves (3 SLSN-I, 2 SN Ia, 1 SN II and 1 TDE with peak magnitude $\sim 17^m$) and used these objects as input to our k-D tree (see Section 3). An example of a ZTF SN Ia simulation is given in Fig. 1.

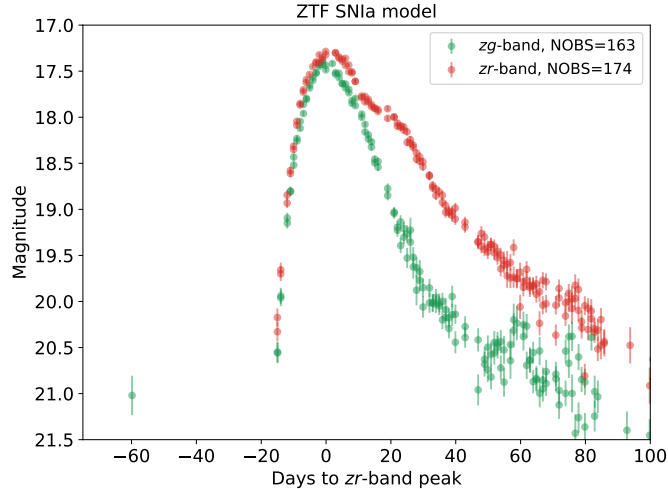


Figure 1: Simulation of an SN Ia used to match with ZTF DR4 data. Green and red circles correspond to zg - and zr -band observations, respectively. Both bands have more than 100 detections with $\text{SNR} > 5$. This simulation’s 8th nearest neighbor via the k-D tree algorithm is SNAD156/AT 2018lzb.

2.3. Light curve selection

ZTF DR4 includes a photometric dataset grouped into objects by a detection position, an observation field, and a passband. Thus, a single stellar source can be represented by multiple objects due to overlapping fields and several observed passbands. We perform $0.2''$ cross-matching to associate different objects as a single source using the ClickHouse database management system⁵. We select observations with `catflags = 0`, positive `magerr`, in zg - & zr -passbands only, and within the first 420 days of the survey. Moreover, we consider objects with the absolute value of the galactic latitude larger than 15 degrees and having at least 100 detections per passband

⁵<https://clickhouse.com>

(non-detections are not presented in ZTF DRs). Finally, we filter out light curves having small variability for which $\frac{1}{N-1} \sum (\frac{m_i - \bar{m}}{\sigma_i})^2 < 3$, where N is the number of observations, m_i and σ_i are detection magnitudes and corresponding error estimates, and $\bar{m} \equiv \sum (m_i / \sigma_i^2) / \sum (1 / \sigma_i^2)$ is a weighted mean magnitude. As a result, we were left with 990,220 sources.

2.4. Pre-processing

We extract light curve features for both simulations and our sample of ZTF DR4 data with the `light-curve`⁶ package (Malanchev et al., 2021). We use a total of 82 light curve features (41 per band) including magnitude amplitude, Stetson K coefficient (Stetson, 1996), standard deviation of Lomb–Scargle periodogram (Lomb, 1976a; Scargle, 1982a), etc. Our list encloses 68 magnitude-based and 14 flux-based features, whereby 66 are brightness-related and 16 are temporally-related; see the complete list in Appendix B.

3. Methodology

We take seven of the brightest simulations (3 SLSN-I, 2 SN Ia, 1 SN II and 1 TDE with peak magnitude $\sim 17^m$) and apply a k-D tree (Bentley, 1975) to their extracted 82 features. Subsequently, we identify the 15 nearest neighbors for each simulation (105 matches in total, resulting in 92 unique ZTF DR4 sources). We inspected their light curves using the SNAD ZTF viewer⁷ (Malanchev et al., 2021), a tool that allows easy access to the individual exposure images; to the Aladin Sky Atlas (Bonnarel et al., 2000; Boch and Fernique, 2014); and to various catalogues of variable stars and transients, including the General Catalogue of Variable Stars (GCVS, Samus’ et al. 2017), the American Association of Variable Star Observers’ Variable Star Index (AAVSO VSX, Watson et al. 2006), the Asteroid Terrestrial-impact Last Alert System (ATLAS, Heinze et al. 2018), the ZTF Catalog of Periodic Variable Stars (Chen et al., 2020), `astrocats`⁸, the OGLE-III Online Catalog of Variable Stars (Soszynski et al., 2008), and the SIMBAD database (Wenger et al., 2000). It also contains the information about object colour and galactic extinction in the chosen direction. Thus, we consider

⁶<https://github.com/light-curve/light-curve>

⁷<https://ztf.snad.space/>

⁸<https://astrocats.space/>

Table 1: Results of transient mining in ZTF DR4 using k-D trees.

Name	R.A.	Dec.	Host galaxy*	z_{ph}	TNS	Type [†]	Comments
SNAD149	284.35219	67.17743			AT 2018lyu	PSN	ZTF18abrlhnm
SNAD150	240.75660	32.64360	SDSS J160301.52+323835.8		AT 2018lyv	PSN	ZTF18aaqnsia
SNAD151	190.61613	52.77285	SDSS J124227.87+524621.9	0.20±0.11	AT 2018lyw	PSN	ZTF19aaoykyz
SNAD152	212.40042	55.95669	SDSS J140936.12+555724.5	0.11±0.03	AT 2018lyx	PSN	ZTF18aanaryv
SNAD153	325.96473	24.35382	SDSS J214351.53+242113.6	0.17±0.04	AT 2018lyy	AGN	ZTF18abvosry
SNAD154	219.40247	38.04782	SDSS J143736.57+380252.0	0.22±0.08	AT 2018lyz	AGN	
SNAD155	212.29492	38.70615	SDSS J140910.77+384222.1	0.39±0.06	AT 2018lza	AGN	ZTF18acwyiyb
SNAD156	184.83691	45.49015	SDSS J121920.85+452924.4	0.09±0.02	AT 2018lzb	PSN	
SNAD157	280.69720	36.36783			AT 2018lzc	PSN	ZTF18abegwmh
SNAD158	253.15763	25.82260	SDSS J165237.84+254921.2	0.14±0.05	AT 2018lzd	AGN	
SNAD159	216.86359	53.08862	SDSS J142727.25+530518.9	0.17±0.07	AT 2018lze	PSN	ZTF19aanjzps

* If available, candidate host galaxies from SDSS DR16 (Ahumada et al., 2020) and their corresponding photometric redshifts (z_{ph}).

† PSN — possible supernova, AGN — active galactic nucleus.

that all publicly available sources were included in our search. If an object was not announced by a survey, we consider it as undiscovered.

The k-D tree takes ~ 6 seconds on a 2 GHz Quad-Core Intel Core i5 processor. Although we use the default Euclidean distance metric for distance, we will explore other distance metrics such as Manhattan and Mahalanobis distances in future work.

4. Results

4.1. Supernova and AGN candidates

As a result of transient mining, we discovered 11 previously unreported supernova and active galactic nucleus candidates (see Table 1). The remaining 94 matches (81 unique ZTF DR4 sources) were either known/already reported transients or variable stars.

Among the 11 new objects, 9 are coincident with galaxy positions cataloged in SDSS DR16 (Ahumada et al., 2020), thus confirming their extragalactic origin. We conclude that 7 of the candidates are likely to be SN and 4 others are AGN candidates (see Fig. A.4). All candidates were sent to the Transient Name Server⁹ (TNS) and received an official TNS identifier as well as an internal SNAD name (Table 1).

⁹<https://www.wis-tns.org/>

Among our discovery objects, **SNAD150**, **SNAD152**, and **SNAD155** occurred when the ZTF template reference image was taken. This detail provides a possible reason for why they were initially unreported, as the ZTF alert stream utilizes differential photometry. Perhaps more importantly, three objects from our list are missing in the official ZTF alert stream, two of which we classify as AGN candidates (**SNAD154**, **SNAD158**) and the third as a possible SN (**SNAD156**). Missed transients **SNAD154** and **SNAD156** have a peak magnitude $\sim 18.5^m - 19.5^m$ which is comparable to those of other SNAD objects listed here but are also detected by the alert system. Moreover, some of our candidates (e.g., **SNAD150**, **SNAD151**) have well-sampled early light curves which could help constrain the progenitor parameters of supernovae and shed light on the explosion scenarios (Jones et al., 2021).

To illustrate the scientific significance of these candidates, we perform light curve fits on two of them, **SNAD150** and **SNAD154**. We use the PYTHON library `SNCOSMO`¹⁰ to fit their light curves with Peter Nugent’s spectral templates¹¹ which cover the main supernova types (Ia, Ib/c, IIP, IIL, IIn). Nugent’s models are simple spectral time series that can be scaled up and down. The zero phase is defined relative to the explosion moment and the observed time t is related to phase via $t = t_0 + \text{phase} \times (1+z)$. Other model parameters are redshift z , observer-frame time corresponding to the zero source’s phase t_0 , and the amplitude.

We extract photometry in zg , zr , and zi passbands from only one field. Then, we subtract the reference magnitude from ZTF light curves to roughly account for the host galaxy contamination. To estimate the redshift bounds for **SNAD150**, we adopt $[-15; -22]$ as an acceptable region for the supernovae absolute magnitude (Richardson et al., 2014) and then, using the apparent maximum magnitude, transform it to the possible redshift range. For **SNAD154** there is a known SDSS galaxy at the source position with measured photometric redshift and corresponding errors, which we use for redshift bounds. Results of the fit are shown in Figs. 2 and 3. **SNAD150** light curves are best described by Nugent’s Type Ia Supernova model, while **SNAD154** is not well fitted by any of them—the observed light curve width near the peak brightness in zg and zr bands is smaller than the models suggest. Thus, we conclude that **SNAD154** object is likely to be an active galactic nucleus.

¹⁰<https://sncosmo.readthedocs.io/en/stable/>

¹¹https://c3.lbl.gov/nugent/nugent_templates.html

5. Conclusions

The consequences of large and complex astronomical datasets have been extensively discussed in the literature. A large part of such discussions focus on the potential of different machine learning algorithms, and are backed by their performance on large simulated datasets. This allows researchers to report on statistical properties of classifiers. In this work, we explored the potential of simulations from a different perspective.

Our analysis relies on two hypotheses: 1) state of the art simulations are a good proxy to real data, and 2) astrophysically inspired features correctly summarize the information necessary to characterize transient light curves. These hypotheses perfectly translate the underlying principles of all SNAD efforts, whose focus is to construct environments that coherently incorporate domain knowledge in learning strategies.

Both statements were tested by extracting the same 82 features from a small number of simulations (7 light curves representing 4 different classes) as well as from real data (ZTF DR4, comprising 990,220 objects). Subsequently, a k-D tree with Euclidean distance was used to search for the 15 objects in real data which were closest match in feature space to each simulation. By visually inspecting 105 total source matches (92 unique), we identified 11 previously unreported transient events, all occurring in 2018. Among these, 7 possible supernovae and 4 AGN candidates, the majority of them with light curves containing several observed epochs before maximum brightness.

In order to estimate how the efficiency of our method is affected by the high number of features (Kung et al., 2001), we also performed the k-D tree analysis in a 15 dimension parameter space resulting from Principal Component Analysis (PCA, Jolliffe, 1986). This dimensionality reduction retains 86% of the variance of our original 82 dimensional parameter space. We obtained results in good agreement (Mira stars, cataclysmic variables, confirmed SN, unconfirmed transients, etc.) with those presented here, including some of the same discovery objects listed in this work (e.g. SNAD150). A detailed analysis of this lower dimensional parameter space and its quantitative impact on our results is an interesting investigation suited for subsequent analysis.

Beyond confirming our initial hypothesis about the importance of simulations and physically inspired features, such results also highlight the importance of further improving observation pipelines and the central role classical learning algorithms can play in this task. Our candidates include 3 objects

which were not part of the ZTF alert stream despite being as bright as the others and holding a considerable number of pre-maximum observations. Given the importance of early detections in astrophysical investigations, and their potential to trigger further spectroscopic follow-up, it is paramount to prevent similar future losses by bringing attention to these missed transient events.

Moreover, we showed that the ZTF DRs can be a fertile ground for testing machine learning pipelines currently being prepared for future large scale surveys. Since we expect transient events to be a small fraction of the total number of objects in the DRs, it provides a perfect environment to stress-test data mining and anomaly detection algorithms, which do not require a large number of labels, before the arrival of LSST.

The era of big data in astronomy has imposed the necessity of automatic learning algorithms in order to digest large and complex datasets. Nevertheless, we should not underestimate the role of domain experts when adapting machines to work in real scientific data environments. Their input is vital to direct changes in the learning strategy due to the expert’s response (e.g. as in active learning algorithms) or in the design of physically motivated features, realistic simulations and physically motivated evaluation criteria. The successful incorporation of this long acquired knowledge to automatic learning frameworks is necessary to ensure we will be able to fully explore the scientific potential of our data.

6. Acknowledgments

The authors thank Vasilisa Malancheva, Anastasia Malancheva, and Vadim Krushinsky for enlightening discussions. We would also like to thank Rick Kessler for his help with ZTF simulations and SNANA.

The reported study was funded by RFBR and CNRS according to the research project № 21-52-15024. SNAD receives financial support from CNRS International Emerging Actions under the project *Real-time analysis of astronomical data for the Legacy Survey of Space and Time* during 2021-2022. The authors acknowledge the support by the Interdisciplinary Scientific and Educational School of Moscow University “Fundamental and Applied Space Research”. P.D.A. is supported by the Center for Astrophysical Surveys at the National Center for Supercomputing Applications (NCSA) as an Illinois Survey Science Graduate Fellow. This research also used resources of the

National Energy Research Scientific Computing Center (NERSC), a U.S. Department of Energy Office of Science User Facility located at Lawrence Berkeley National Laboratory, operated under Contract No. DE-AC02-05CH11231.

This manuscript has been authored by employees of Brookhaven Science Associates, LLC under Contract No. DE-SC0012704 with the U.S. Department of Energy. The publisher by accepting the manuscript for publication acknowledges that the United States Government retains a non-exclusive, paid-up, irrevocable, world-wide license to publish or reproduce the published form of this manuscript, or allow others to do so, for United States Government purposes.

This research has made use of NASA’s Astrophysics Data System Bibliographic Services and following Python software packages: NUMPY (van der Walt et al., 2011), MATPLOTLIB (Hunter, 2007), SCIPLY (Jones et al., 2001), PANDAS (pandas development team, 2020; Wes McKinney, 2010), SCIKIT-LEARN (Pedregosa et al., 2011), ASTROPY (Astropy Collaboration et al., 2013, 2018), and ASTROQUERY (Ginsburg et al.).

References

- Ahumada, R., Allende Prieto, C., Almeida, A., et al., 2020. The 16th Data Release of the Sloan Digital Sky Surveys: First Release from the APOGEE-2 Southern Survey and Full Release of eBOSS Spectra. *ApJS* 249, 3. doi:10.3847/1538-4365/ab929e, arXiv:1912.02905.
- Aleo, P.D., Ishida, E.E.O., Kornilov, M., et al., 2020. The Most Interesting Anomalies Discovered in ZTF DR3 from the SNAD-III Workshop. *Research Notes of the American Astronomical Society* 4, 112. doi:10.3847/2515-5172/aba6e8.
- Allam, Tarek, J., McEwen, J.D., 2021. Paying Attention to Astronomical Transients: Photometric Classification with the Time-Series Transformer. arXiv e-prints , arXiv:2105.06178arXiv:2105.06178.
- Alves, C.S., Peiris, H.V., Lochner, M., McEwen, J.D., Allam, Tarek, J., Biswas, R., 2021. Considerations for optimizing photometric classification of supernovae from the Rubin Observatory. arXiv e-prints , arXiv:2107.07531arXiv:2107.07531.
- Astropy Collaboration, Price-Whelan, A.M., SipHocz, B.M., et al., 2018. The Astropy Project: Building an Open-science Project and Status of the

- v2.0 Core Package. *The Astronomical Journal* 156, 123. doi:10.3847/1538-3881/aabc4f, arXiv:1801.02634.
- Astropy Collaboration, Robitaille, T.P., Tollerud, E.J., et al., 2013. Astropy: A community Python package for astronomy. *Astronomy and Astrophysics* 558, A33. doi:10.1051/0004-6361/201322068, arXiv:1307.6212.
- Bellm, E.C., Kulkarni, S.R., Graham, M.J., et al., 2019. The Zwicky Transient Facility: System Overview, Performance, and First Results. *Publications of the Astronomical Society of the Pacific* 131, 018002. doi:10.1088/1538-3873/aaecbe, arXiv:1902.01932.
- Bentley, J.L., 1975. Multidimensional binary search trees used for associative searching. *Commun. ACM* 18, 509–517. URL: <https://doi.org/10.1145/361002.361007>, doi:10.1145/361002.361007.
- Boch, T., Fernique, P., 2014. Aladin Lite: Embed your Sky in the Browser, in: Manset, N., Forshay, P. (Eds.), *Astronomical Data Analysis Software and Systems XXIII*, p. 277.
- Bonnarel, F., Fernique, P., Bienaymé, O., et al., 2000. The ALADIN interactive sky atlas. A reference tool for identification of astronomical sources. *A&AS* 143, 33–40. doi:10.1051/aas:2000331.
- Boone, K., 2019. Avocado: Photometric Classification of Astronomical Transients with Gaussian Process Augmentation. *AJ* 158, 257. doi:10.3847/1538-3881/ab5182, arXiv:1907.04690.
- Burhanudin, U.F., Maund, J.R., Killestein, T., et al., 2021. Light-curve classification with recurrent neural networks for GOTO: dealing with imbalanced data. *MNRAS* 505, 4345–4361. doi:10.1093/mnras/stab1545, arXiv:2105.11169.
- Chatterjee, D., Narayan, G., Aleo, P.D., et al., 2021. El-CID: A filter for Gravitational-wave Electromagnetic Counterpart Identification. arXiv e-prints, arXiv:2108.04166arXiv:2108.04166.
- Chen, X., Wang, S., Deng, L., et al., 2020. The Zwicky Transient Facility Catalog of Periodic Variable Stars. *ApJS* 249, 18. doi:10.3847/1538-4365/ab9cae, arXiv:2005.08662.

- D’Isanto, A., Cavuoti, S., Brescia, M., et al., 2016. An analysis of feature relevance in the classification of astronomical transients with machine learning methods. *Monthly Notices of the Royal Astronomical Society* 457, 3119–3132. doi:10.1093/mnras/stw157, arXiv:1601.03931.
- Ginsburg, A., Sipócz, B.M., Brasseur, C.E., Cowperthwaite, P.S., et al., .
- Graham, M.J., Kulkarni, S.R., Bellm, E.C., et al., 2019. The zwicky transient facility: Science objectives. *Publications of the Astronomical Society of the Pacific* 131, 078001. URL: <https://doi.org/10.1088/1538-3873/ab006c>, doi:10.1088/1538-3873/ab006c.
- Heinze, A.N., Tonry, J.L., Denneau, L., et al., 2018. A First Catalog of Variable Stars Measured by the Asteroid Terrestrial-impact Last Alert System (ATLAS). *The Astronomical Journal* 156, 241. doi:10.3847/1538-3881/aae47f, arXiv:1804.02132.
- Hložek, R., Ponder, K.A., Malz, A.I., et al., 2020. Results of the Photometric LSST Astronomical Time-series Classification Challenge (PLAsTiCC). arXiv e-prints , arXiv:2012.12392arXiv:2012.12392.
- Hunter, J.D., 2007. Matplotlib: A 2D Graphics Environment. *Computing in Science and Engineering* 9, 90–95. doi:10.1109/MCSE.2007.55.
- Ishida, E.E.O., Beck, R., González-Gaitán, S., et al., 2019a. Optimizing spectroscopic follow-up strategies for supernova photometric classification with active learning. *MNRAS* 483, 2–18. doi:10.1093/mnras/sty3015, arXiv:1804.03765.
- Ishida, E.E.O., Kornilov, M.V., Malanchev, K.L., et al., 2019b. Active Anomaly Detection for time-domain discoveries. arXiv e-prints , arXiv:1909.13260arXiv:1909.13260.
- Ishida, E.E.O., Kornilov, M.V., Malanchev, K.L., et al., 2021. Active anomaly detection for time-domain discoveries. *A&A* 650, A195. doi:10.1051/0004-6361/202037709, arXiv:1909.13260.
- Jolliffe, I.T., 1986. *Principal Component Analysis and Factor Analysis*. Springer New York, New York, NY. pp. 115–128. URL: https://doi.org/10.1007/978-1-4757-1904-8_7, doi:10.1007/978-1-4757-1904-8_7.

- Jones, D.O., Foley, R.J., Narayan, G., et al., 2021. The Young Supernova Experiment: Survey Goals, Overview, and Operations. *ApJ* 908, 143. doi:10.3847/1538-4357/abd7f5, arXiv:2010.09724.
- Jones, E., Oliphant, T., Peterson, P., et al., 2001. SciPy: Open source scientific tools for Python. URL: <http://www.scipy.org/>. [Online; accessed `today`].
- Kenamer, N., Ishida, E.E.O., González-Gaitán, S., et al., 2020. Active learning with respect: Resource allocation for extragalactic astronomical transients, in: 2020 IEEE Symposium Series on Computational Intelligence (SSCI), pp. 3115–3124. doi:10.1109/SSCI47803.2020.9308300.
- Kessler, R., Bassett, B., Belov, P., et al., 2010. Results from the Supernova Photometric Classification Challenge. *PASP* 122, 1415. doi:10.1086/657607, arXiv:1008.1024.
- Kessler, R., Bernstein, J.P., Cinabro, D., et al., 2009. SNANA: A Public Software Package for Supernova Analysis. *PASP* 121, 1028. doi:10.1086/605984, arXiv:0908.4280.
- Kessler, R., Narayan, G., Avelino, A., et al., 2019. Models and Simulations for the Photometric LSST Astronomical Time Series Classification Challenge (PLAsTiCC). *PASP* 131, 094501. doi:10.1088/1538-3873/ab26f1, arXiv:1903.11756.
- Kim, D.W., Protopapas, P., Bailer-Jones, C.A.L., et al., 2014. The EPOCH Project. I. Periodic variable stars in the EROS-2 LMC database. *Astronomy and Astrophysics* 566, A43. doi:10.1051/0004-6361/201323252, arXiv:1403.6131.
- Krone-Martins, A., Moitinho, A., 2014. UPMASK: unsupervised photometric membership assignment in stellar clusters. *A&A* 561, A57. doi:10.1051/0004-6361/201321143, arXiv:1309.4471.
- Kung, S.Y., Larsen, J., Guan, L., 2001. Multimedia image and video processing / edited by Ling Guan, Sun-Yuan Kung, Jan Larsen. CRC Press Boca Raton, Fla.

- Lochner, M., McEwen, J.D., Peiris, H.V., Lahav, O., Winter, M.K., 2016. Photometric Supernova Classification with Machine Learning. *ApJS* 225, 31. doi:10.3847/0067-0049/225/2/31, arXiv:1603.00882.
- Lomb, N.R., 1976a. Least-Squares Frequency Analysis of Unequally Spaced Data. *Ap&SS* 39, 447–462. doi:10.1007/BF00648343.
- Lomb, N.R., 1976b. Least-Squares Frequency Analysis of Unequally Spaced Data. *Astrophysics and Space Science* 39, 447–462. doi:10.1007/BF00648343.
- LSST Science Collaboration, Abell, P.A., Allison, J., et al., 2009. LSST Science Book, Version 2.0. ArXiv e-prints arXiv:0912.0201.
- Malanchev, K.L., Pruzhinskaya, M.V., Korolev, V.S., et al., 2021. Anomaly detection in the Zwicky Transient Facility DR3. *MNRAS* 502, 5147–5175. doi:10.1093/mnras/stab316, arXiv:2012.01419.
- Martínez-Galarza, J.R., Bianco, F.B., Crake, D., Tirumala, K., Mahabal, A.A., Graham, M.J., Giles, D., 2021. A method for finding anomalous astronomical light curves and their analogs. *MNRAS* doi:10.1093/mnras/stab2588, arXiv:2009.06760.
- Matheson, T., Stubens, C., Wolf, N., Lee, C.H., Narayan, G., Saha, A., Scott, A., Soraisam, M., Bolton, A.S., Hauger, B., Silva, D.R., Kececioglu, J., Scheidegger, C., Snodgrass, R., Aleo, P.D., Evans-Jacquez, E., Singh, N., Wang, Z., Yang, S., Zhao, Z., 2021. The ANTARES Astronomical Time-domain Event Broker. *AJ* 161, 107. doi:10.3847/1538-3881/abd703, arXiv:2011.12385.
- Wes McKinney, 2010. Data Structures for Statistical Computing in Python, in: Stéfan van der Walt, Jarrod Millman (Eds.), *Proceedings of the 9th Python in Science Conference*, pp. 56 – 61. doi:10.25080/Majora-92bf1922-00a.
- Möller, A., Peloton, J., Ishida, E.E.O., et al., 2020. Fink, a new generation of broker for the LSST community. arXiv e-prints , arXiv:2009.10185arXiv:2009.10185.
- Möller, A., Peloton, J., Ishida, E.E.O., Arnault, C., Bachelet, E., Blaineau, T., Boutigny, D., Chauhan, A., Gangler, E., Hernandez, F., Hrivnac, J.,

- Leoni, M., Leroy, N., Moniez, M., Pateyron, S., Ramparison, A., Turpin, D., Ansari, R., Allam, Tarek, J., Bajat, A., Biswas, B., Boucaud, A., Bregeon, J., Campagne, J.E., Cohen-Tanugi, J., Coleiro, A., Dornic, D., Fouchez, D., Godet, O., Gris, P., Karpov, S., Nebot Gomez-Moran, A., Neveu, J., Plaszczyński, S., Savchenko, V., Webb, N., 2021. FINK, a new generation of broker for the LSST community. *MNRAS* 501, 3272–3288. doi:10.1093/mnras/staa3602, arXiv:2009.10185.
- Muthukrishna, D., Mandel, K.S., Lochner, M., Webb, S., Narayan, G., 2021. Real-time detection of anomalies in large-scale transient surveys. arXiv e-prints , arXiv:2111.00036arXiv:2111.00036.
- Muthukrishna, D., Narayan, G., Mandel, K.S., et al., 2019. RAPID: Early Classification of Explosive Transients Using Deep Learning. *PASP* 131, 118002. doi:10.1088/1538-3873/ab1609, arXiv:1904.00014.
- Pasquet, J., Pasquet, J., Chaumont, M., et al., 2019. PELICAN: deeP architecture for the LIght Curve ANalysis. *A&A* 627, A21. doi:10.1051/0004-6361/201834473, arXiv:1901.01298.
- Pedregosa, F., Varoquaux, G., Gramfort, A., et al., 2011. Scikit-learn: Machine learning in Python. *Journal of Machine Learning Research* 12, 2825–2830.
- Pera, M.S., Perren, G.I., Moitinho, A., et al., 2021. pyUPMASK: an improved unsupervised clustering algorithm. *A&A* 650, A109. doi:10.1051/0004-6361/202040252, arXiv:2101.01660.
- Perlmutter, S., Aldering, G., Goldhaber, G., et al., 1999. Measurements of Ω and Λ from 42 High-Redshift Supernovae. *ApJ* 517, 565–586. doi:10.1086/307221, arXiv:astro-ph/9812133.
- Pruzhinskaya, M.V., Malanchev, K.L., Kornilov, M.V., et al., 2019. Anomaly detection in the Open Supernova Catalog. *Monthly Notices of the Royal Astronomical Society* 489, 3591–3608. doi:10.1093/mnras/stz2362, arXiv:1905.11516.
- Ralph, N.O., Norris, R.P., Fang, G., et al., 2019. Radio Galaxy Zoo: Unsupervised Clustering of Convolutionally Auto-encoded Radio-astronomical Images. *PASP* 131, 108011. doi:10.1088/1538-3873/ab213d, arXiv:1906.02864.

- Richardson, D., Jenkins, Robert L., I., Wright, J., et al., 2014. Absolute-magnitude Distributions of Supernovae. *AJ* 147, 118. doi:10.1088/0004-6256/147/5/118, arXiv:1403.5755.
- Riess, A.G., Filippenko, A.V., Challis, P., et al., 1998. Observational Evidence from Supernovae for an Accelerating Universe and a Cosmological Constant. *AJ* 116, 1009–1038. doi:10.1086/300499, arXiv:astro-ph/9805201.
- Sadeh, I., 2020. Data-driven Detection of Multimessenger Transients. *ApJ* 894, L25. doi:10.3847/2041-8213/ab8b5f, arXiv:2005.06406.
- Samus', N.N., Kazarovets, E.V., Durlevich, O.V., et al., 2017. General catalogue of variable stars: Version GCVS 5.1. *Astronomy Reports* 61, 80–88. doi:10.1134/S1063772917010085.
- Sánchez, P., Lira, P., Cartier, R., Pérez, V., Miranda, N., Yovaniniz, C., Arévalo, P., Milvang-Jensen, B., Fynbo, J., Dunlop, J., Coppi, P., Marchesi, S., 2017. Near-infrared Variability of Obscured and Unobscured X-Ray-selected AGNs in the COSMOS Field. *ApJ* 849, 110. doi:10.3847/1538-4357/aa9188, arXiv:1710.01306.
- Scargle, J.D., 1982a. Studies in astronomical time series analysis. II. Statistical aspects of spectral analysis of unevenly spaced data. *ApJ* 263, 835–853. doi:10.1086/160554.
- Scargle, J.D., 1982b. Studies in astronomical time series analysis. II. Statistical aspects of spectral analysis of unevenly spaced data. *The Astrophysical Journal* 263, 835–853. doi:10.1086/160554.
- Sooknunan, K., Lochner, M., Bassett, B.A., Peiris, H.V., Fender, R., Stewart, A.J., Pietka, M., Woudt, P.A., McEwen, J.D., Lahav, O., 2021. Classification of multiwavelength transients with machine learning. *MNRAS* 502, 206–224. doi:10.1093/mnras/staa3873, arXiv:1811.08446.
- Soszynski, I., Poleski, R., Udalski, A., et al., 2008. The Optical Gravitational Lensing Experiment. The OGLE-III Catalog of Variable Stars. I. Classical Cepheids in the Large Magellanic Cloud. *Acta Astron.* 58, 163–185. arXiv:0808.2210.

- Stetson, P.B., 1996. On the Automatic Determination of Light-Curve Parameters for Cepheid Variables. *Publications of the Astronomical Society of the Pacific* 108, 851. doi:10.1086/133808.
- Storey-Fisher, K., Huertas-Company, M., Ramachandra, N., et al., 2021. Anomaly detection in Hyper Suprime-Cam galaxy images with generative adversarial networks. *MNRAS* doi:10.1093/mnras/stab2589, arXiv:2105.02434.
- pandas development team, T., 2020. pandas-dev/pandas: Pandas. URL: <https://doi.org/10.5281/zenodo.3509134>, doi:10.5281/zenodo.3509134.
- van der Walt, S., Colbert, S.C., Varoquaux, G., 2011. The NumPy Array: A Structure for Efficient Numerical Computation. *Computing in Science and Engineering* 13, 22–30. doi:10.1109/MCSE.2011.37, arXiv:1102.1523.
- Villar, V.A., Cranmer, M., Berger, E., Contardo, G., Ho, S., Hosseinzadeh, G., Lin, J.Y.Y., 2021. A Deep-learning Approach for Live Anomaly Detection of Extragalactic Transients. *ApJS* 255, 24. doi:10.3847/1538-4365/ac0893, arXiv:2103.12102.
- Villar, V.A., Hosseinzadeh, G., Berger, E., et al., 2020. SuperRAENN: A Semisupervised Supernova Photometric Classification Pipeline Trained on Pan-STARRS1 Medium-Deep Survey Supernovae. *ApJ* 905, 94. doi:10.3847/1538-4357/abc6fd, arXiv:2008.04921.
- Watson, C.L., Henden, A.A., Price, A., 2006. The International Variable Star Index (VSX). *Society for Astronomical Sciences Annual Symposium* 25, 47.
- Wenger, M., Ochsenbein, F., Egret, D., et al., 2000. The SIMBAD astronomical database. The CDS reference database for astronomical objects. *Astronomy and Astrophysics Supplements* 143, 9–22. doi:10.1051/aas:2000332, arXiv:astro-ph/0002110.

Appendix A. ZTF DR4 light curves

Light curves of 11 newly found transients, generated with the ZTF SNAD viewer. The plots show only data from ZTF DR4 used for feature extraction (Section 2.4).

Appendix B. Light-curve features

We extract 41 light-curve features for each of zg - and zr -passbands using the `light-curve-feature` Rust crate (Malanchev et al., 2021)¹². We use the following feature extractors:

- a magnitude amplitude;
- a magnitude standard deviation;
- kurtosis of magnitude and flux distributions, two features;
- skews of magnitude and flux distributions, two features;
- Anderson–Darling test of normality statistics values for magnitudes and fluxes, two features;
- a fraction of observations beyond one/two standard deviations from mean magnitude (D’Isanto et al., 2016), two features;
- a range of cumulative sums of magnitudes and fluxes (Kim et al., 2014), two features;
- a magnitude inter-percentile ranges 2% – 98%, 10% – 90% and 25% – 75%, three features;
- a slope and its error of a linear fit of a magnitude light curve with and without respect to the observation errors, four features;
- a ratio of magnitude inter-percentile ranges: 1) 40% – 60% to 5% – 95% and 2) 20% – 80% to 5% – 95% (D’Isanto et al., 2016), two features;
- a mean magnitude value with and without respect to the observation errors, two features;
- a median of the absolute value of the difference between magnitude and median of magnitude distribution (D’Isanto et al., 2016);
- a fraction of observations being within 0.1/0.2 magnitude amplitude from median magnitude (D’Isanto et al., 2016), two features;

¹²See detailed feature description and package documentation on <https://docs.rs/light-curve-feature/0.2.2/>

- the maximum deviation of magnitude from median magnitude (D’Isanto et al., 2016);
- a ratio of 5% – 95%/10% – 90% magnitude inter-percentile range to the median magnitude (D’Isanto et al., 2016), two features;
- signal-to-noise ratio of five largest Lomb–Scargle periodogram peaks, periodogram power standard deviation, and a fraction of periodogram points beyond two/three standard deviations from the mean power value, (Lomb, 1976b; Scargle, 1982b; D’Isanto et al., 2016), eight features;
- the Stetson K coefficient for magnitudes and fluxes (Stetson, 1996), two features;
- an excess variance of fluxes (Sánchez et al., 2017),
- a ratio of flux standard deviation to its mean.

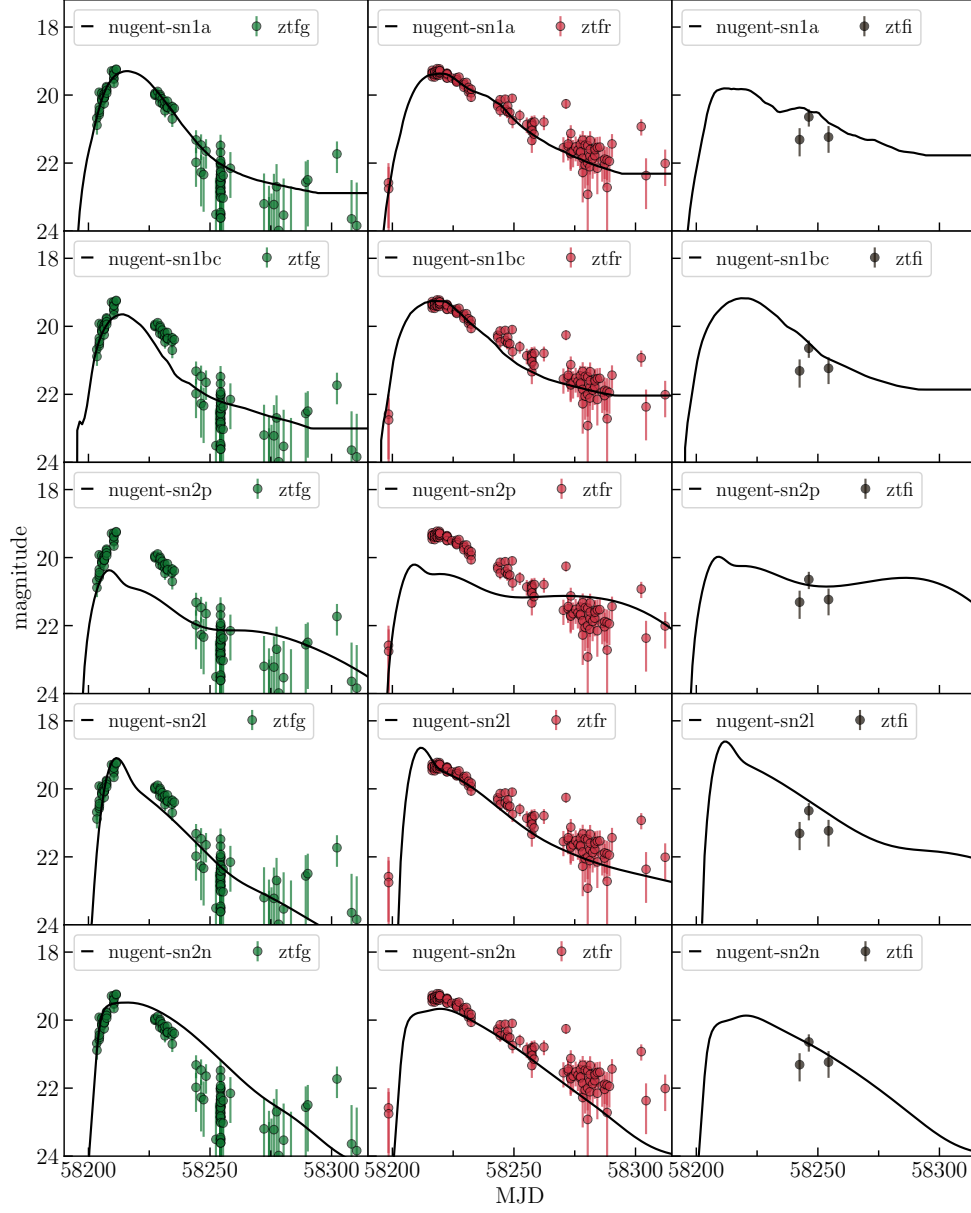


Figure 2: Results of light curve fit of SNAD150 by Nugent's supernova models. Observational data correspond to OIDs: 679108100003227 (*zg*), 679208100014706 (*zr*), 679308100021192 (*zi*).

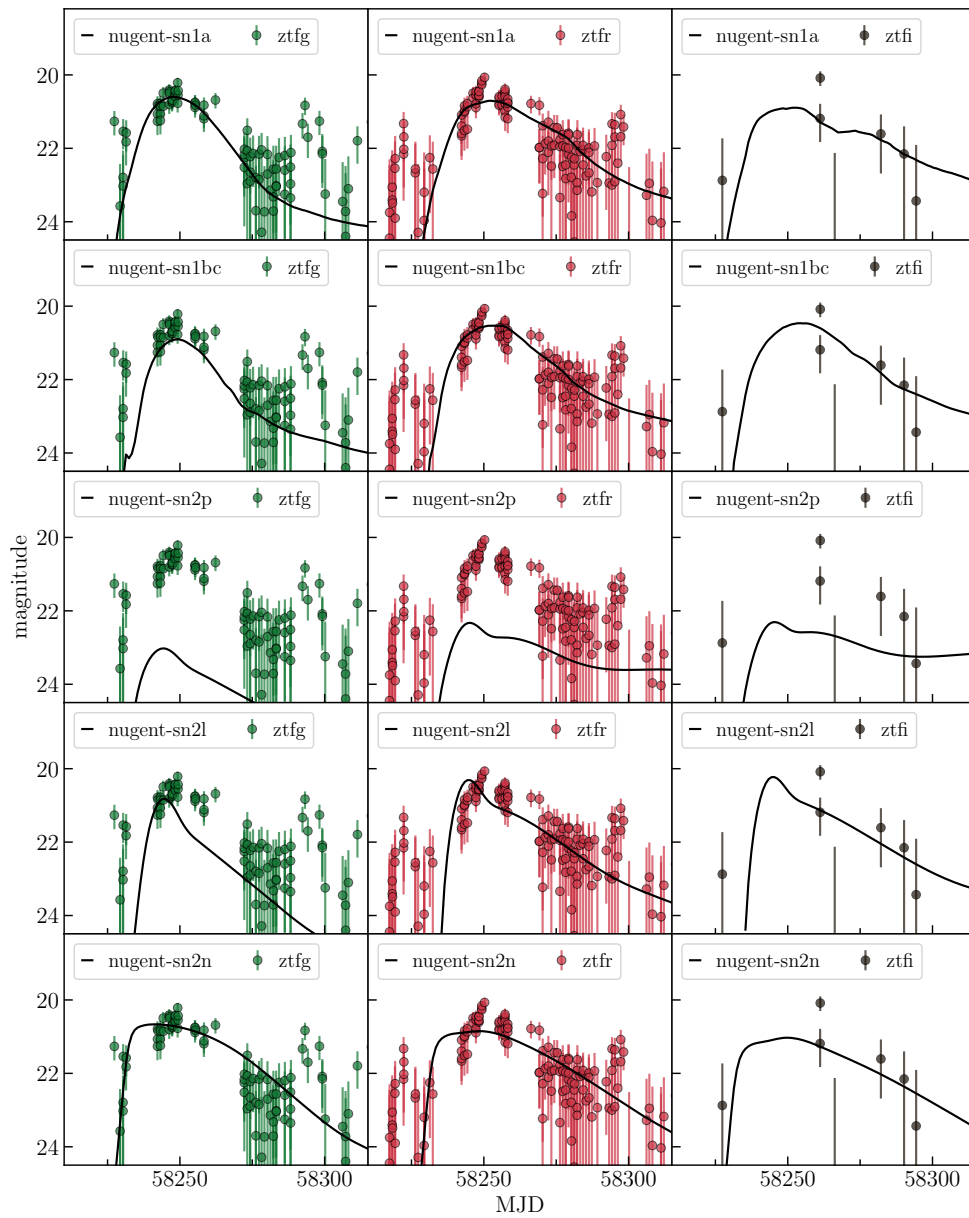
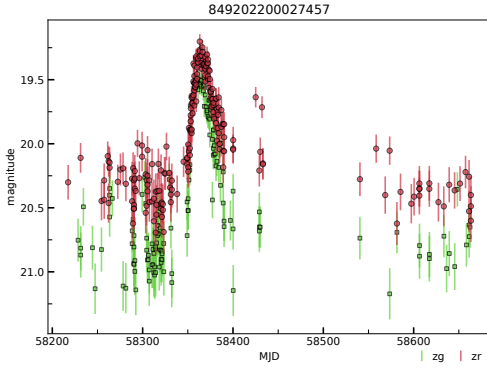
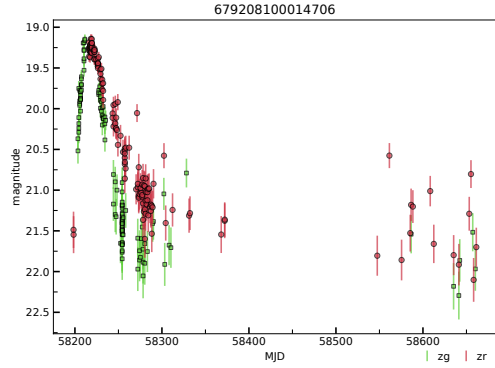


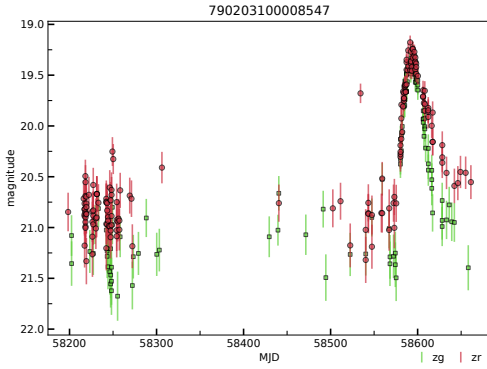
Figure 3: Results of light curve fit of SNAD154 by Nugent's supernova models. Observational data correspond to OIDs: 719102100006086 (zg), 719202100004008 (zr), 719302100018848 (zi).



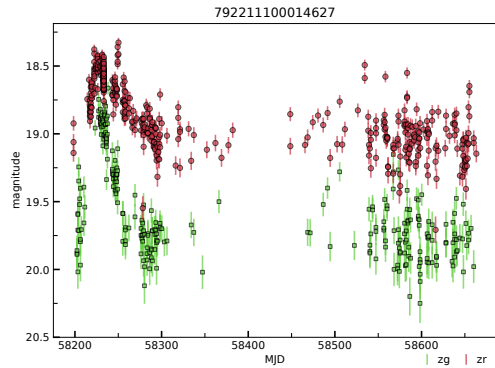
a) SNAD149: 849102200015533 (*zg*),
849202200027457 (*zr*)



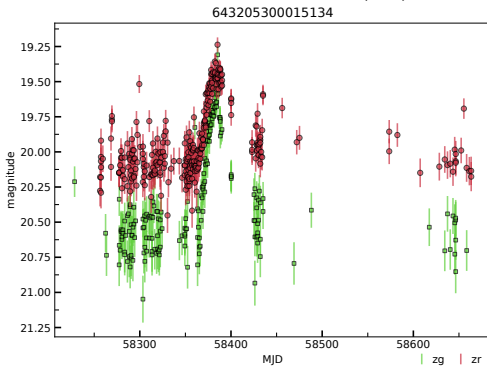
b) SNAD150: 679108100003227 (*zg*),
679208100014706 (*zr*)



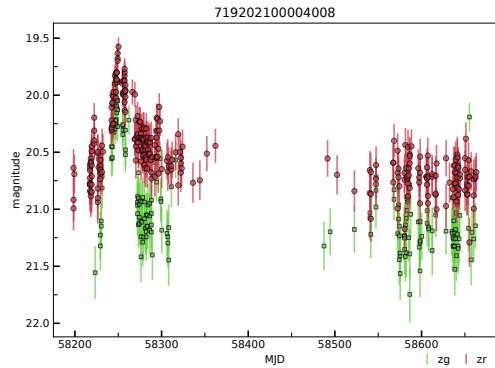
c) SNAD151: 790103100000915 (*zg*),
790203100008547 (*zr*),
1792109200005099 (*zg*)



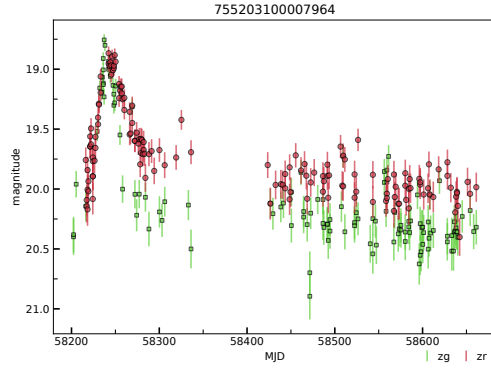
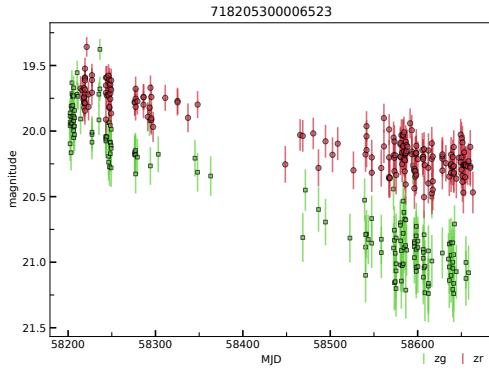
d) SNAD152: 792111100012457 (*zg*),
792211100014627 (*zr*)



e) SNAD153: 643105300009229 (*zg*),
643205300015134 (*zr*)

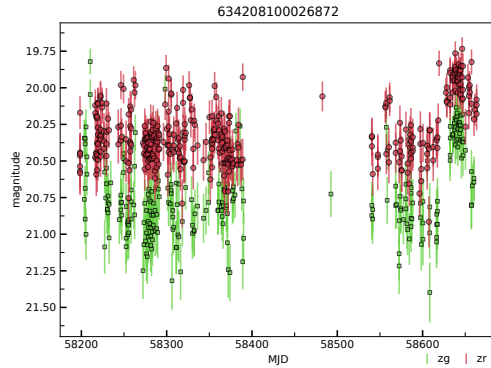
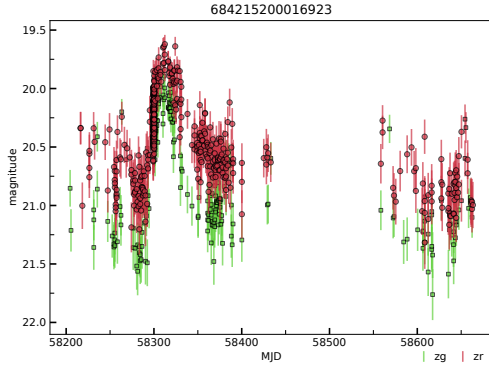


f) SNAD154: 719102100006086 (*zg*),
719202100004008 (*zr*)



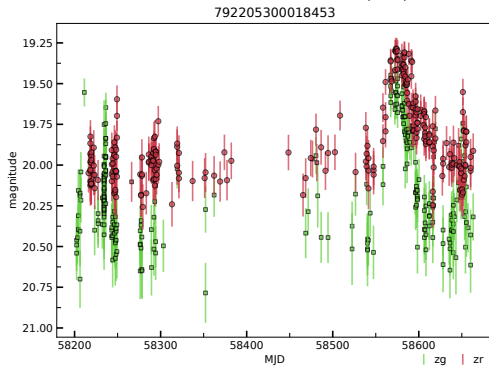
g) SNAD155: 718105300007353 (*zr*),
718205300006523 (*zg*),
1717111100000191 (*zr*)

h) SNAD156: 755103100026105 (*zg*),
755203100007964 (*zr*)



i) SNAD157: 684115200018744 (*zg*),
684215200016923 (*zr*),
1725206200027715 (*zr*)

j) SNAD158: 634108100006647 (*zg*),
634208100026872 (*zr*)



k) SNAD159: 792105300007593 (*zg*),
792205300018453 (*zr*),
1795111100013935 (*zg*),
1795211100000534 (*zr*)

Figure A.4: SN/AGN candidate light curves in *zr*- and *zg*-bands within the first 420 days of ZTF DR4, generated with the ZTF SNAD viewer.